Intelligent Precision Control for Haptic Microrobotic Cell Injection System

Ali Ghanbari, XiaoQi Chen, and Wenhui Wang

Department of Mechanical Engineering
University of Canterbury
Christchurch, New Zealand
ali.ghanbari@pg.canterbury.ac.nz

Abstract

Integration of the operator's haptic sensory modality in microrobotic cell injection offers immense benefits over conventional techniques. In particular, the haptically enabled system should be able to manipulate the microrobot in micro resolution. This requires a precision control strategy capable of tracking the trajectory mapped from the haptic side. As the system has an unknown internal structure with nonlinear behavior, an intelligent dynamic modelling and control scheme is developed. Neuro-Fuzzy Inference System (ANFIS) and direct inverse learning method are employed for system identification and control. Experimental results demonstrate that the developed intelligent controller is able to control the microrobotic system with high precision and speed superior to the conventional control methods.

1 Introduction

The literature [Fanning, 2006; Beretta *et al.*, 2006] indicates significant research interest in being able to deposit certain amount of materials such as protein, sperm, DNA and bio-molecules into the specific locations of biological cells and studying cells responses.

Conventionally, cell micro-injection is conducted manually by a trained bio-operator in biological laboratories. Typically, it takes around a year to train a bio-operator to be able to conduct such an operation. However, the success rate is often low [Scherp and Hasenstein, 2003; Tran *et al.*, 2003]. A successful injection is largely dependent on injection accuracy which is very reluctant due to the performance of bio-operator as a human.

The biological micro-manipulation operations have their special specification. The cells, as the manipulated objects, vary in size, shape and biophysical characteristics. The contact forces span a range of μN to mN [Kasaya *et al.*, 1999] and system model is not constant for different experimental conditions. Accordingly, it is highly advantageous to provide more information of the process to the bio-operator while performing the operation, so that cell injection can be more successful. Utilising computer vision to provide visual feedback [Ghanbari *et al.*, 2009a] and measuring the injection force are two examples in this regard [Faramarzi *et al.*, 2009].

We are developing a novel haptic microrobotic cell injection system which provides an enhanced HMI (Human Machine Interface) tool for the bio-operator. This includes haptic-microrobot kinematic mapping strategy to allow the bio-operator to utilise the haptic device to intuitively move the micropipette using a similar method to that of hand-held needle insertion [Ghanbari *et al.*, 2009b] and then introducing haptic virtual fixtures to provide the bio-operator with valuable haptic assistance [Ghanbari, *et al.*, 2010a]. Haptic virtual fixtures provide assistance to the human operator through force and position signals [Ghanbari, *et al*., 2010b].

The term haptic relates to the human's ability to feel. Haptic technologies interact with the human's haptic modality through tactual, force-based or proprioceptive interaction. They have been utilised in a range of applications including virtual manipulation, procedural operator training [Balijepalli and Kesavadas, 2004], mobile robotic teleportation [Horan *et al.*, 2008a; Horan *et al.*, 2008b], and medical simulation and training [Basdogan *et al.*, 2004].

The novelty of our developing system lies in two distinct aspects:

1) The provision of an intuitive method to control the micropipette with direct 3D position to position mapping from the haptic device. This gives rise to the following benefits:
   - *Intuitive needle control:* It provides the ability of moving the micropipette in a similar fashion to conventional handheld needle insertion instead of using the rotary encoder or joystick which normally positions one single axis in one time. It facilitates the interaction of the bio-operator with the micromanipulator. So, it allows the bio-operators to maintain their operation habits, which shortens the training curve.
   - *Guidance:* The operator is guided while performing the injection task via the haptic interface.
   - *Force information:* It provides the basis for the force feedback in the bio-operator's hand.
2) The bio-operator can be trained virtually using the control method presented in this paper with or without the ability to acquire the appropriate real-time sensory information.

In order to implement the desired position-to-position kinematic mapping, it is necessary to continually reposition the micromanipulator from the current position to the desired position. Achieving this requires the micromanipulator control system to track the trajectory of the haptic device of constantly varying velocity. This paper presents a control system designed to continually reposition the micromanipulator's three actuated axes whilst maintaining micro precision.

In order to design such a controller, an accurate model of the system is required. The micromanipulator system exhibits non-linear behaviour and has an unknown internal structure. To overcome these limitations nonlinear system identification methods with black box approaches were investigated. Given the nature of the proposed system, the model required micron resolution accuracy. Non-linear system identification techniques such as Hammerstein-Wiener's blind model identification approach [Bai, 2002] were investigated but found ineffective in achieving desired accuracy.

ANNs (artificial neural networks) and FISs (fuzzy inference systems) are universal approximators. NFSs (neuro-fuzzy systems) which combine the advantages of fuzzy and neuro-learning have become a popular solution to modeling problems. Integration of ANN and FIS combines the advantages of symbolic and numerical processing [Nauck *et al*., 1997].

NFS was first introduced in the late 1980s and the 1990s saw the development of diverse approaches. These approaches can be categorized to three classes of cooperative, concurrent and fused [Vieira *et al.*, 2004]. The most common class is the fused NFS which employs an ANN to train internal parameters of a fuzzy structure. Notably Jang [Jang, 1993] introduced a fused NFS architecture: ANFIS (adaptive neuro-fuzzy inference system) able to approximate linear and non-linear functions (universal approximator).

Intelligent control has been proven to be a practical alternative to conventional control schemes [Denai *et al*., 2004]. This is because fuzzy control and neural network-based control systems are able to deal more effectively with variations of parameters, uncertainty and the unknown structure of the system under control. This results in improved robustness of the control system. A fuzzy control scheme can be enhanced to an adaptive network controller (ANFIS) providing the advantages of ANNs and fuzzy control schemes [Jang and Chuen-Tsai, 2002].

This paper addresses neuro-fuzzy modelling and control of the microrobotic system based on ANFIS. The paper is organized in the following manner. First, ANFIS architecture and learning algorithms are reviewed in brief. Second, microrobotic cell injection system setup is introduced. Next, system identification process is described and modelling results are demonstrated. Finally, Neuro-fuzzy controller system design and experimental results are presented.

2 Adaptive Neuro-Fuzzy Inference System

ANFIS presents an appropriate combination of ANN and FIS. The theory relating to FISs propose that different fuzzification and defuzzification methods as well as different rule bases can propose diverse solutions to a particular task [Jang *et al.*, 1997]. Consider two fuzzy rules of Takagi and Sugeno's type as:

$$\begin{aligned} &\textit{Rule 1:}\quad \text{If } x \text{ is } A_1 \text{ and y is } B_1, \text{ then } \quad f_1 = p_1x+q_1y+r_1 \\ &\textit{Rule 2:}\quad \text{If } x \text{ is } A_2 \text{ and y is } B_2, \text{ then } \quad f_2 = p_2x+q_2y+r_2 \end{aligned} \tag{1}$$

where, x and y are inputs, f is the output, $\{A_i, B_i\}_{i=1,2}$ is linguistic label set, and $\{p_i, q_i, r_i\}_{i=1,2}$ is the parameter set. Then, type-3 ANFIS architecture with first-order Sugeno fuzzy inference system [Takagi and Sugeno, 1985] would be illustrated as Figure 1 (a).

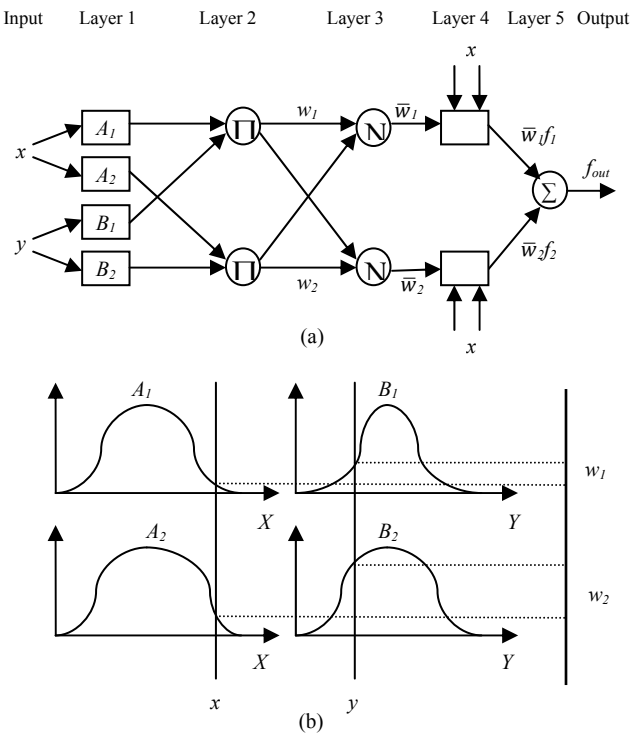

Figure 1. (a) ANFIS architecture; (b) Fuzzy inference mechanism

Figure 1 (b) demonstrates the fuzzy reasoning mechanism which infers output f from input vector $[x,y]$. The firing strengths w_1 and w_2 are calculated as the product of the membership grades of the parameters. Then, system output is obtained as the weighted average of each rule's output. More precisely, the output f can be calculated as

$$f = \frac{w_1f_1+w_2f_2}{w_1+w_2} = \bar{w}_1f_1 + \bar{w}_2f_2 \tag{2}$$

, or

$$f = \frac{\mu_{A_1}(x)\mu_{B_1}(y)(p_1x+q_1y+r_1) + \mu_{A_2}(x)\mu_{B_2}(y)(p_2x+q_2y+r_2)}{\mu_{A_1}(x)\mu_{B_1}(y) + \mu_{A_2}(x)\mu_{B_2}(y)}$$

where $\mu_{A_1}(x), \mu_{B_1}(y), \mu_{A_2}(x)$, and $\mu_{B_2}(y)$ are membership grades of A_1, B_1, A_2 and B_2 respectively.

ANFIS Network is consisted of 5 layers. Square and circle node symbols represent functional and operational nodes respectively. Network lines do not carry any weight and are just responsible to transfer values to the next layer. Briefly, layer 1 calculates the membership grades; layer 2 combines them to form the firing strengths; layer 3 normalizes them; layer 4 constructs the contribution from each rule; and layer 5 generates the final output.

There are two sets of parameters in ANFIS network namely, premise and consequent parameters. Layer 4 parameters are linear. Thus, LSE method is applied to identify them. In contract, layer 1 parameters are

nonlinear. So, the back-propagation gradient decent is used to update them. This is called hybrid learning algorithm which combines the gradient decent and the LSE methods to train the ANFIS network. Each epoch of the learning algorithm is performed in two passes:

- *Forward pass:* input data are supplied and functional signals go forward up to layer 4 to calculate each node output and identifying consequent parameters by LSE method.
- *Backward pass:* error rates propagate backward and the premise parameters are updated by the gradient descent method.

Detailed explanation of ANFIS layers, premise and consequent parameters and hybrid learning algorithm are described in [Ghanbari *et al*., 2009c] previously and thus omitted.

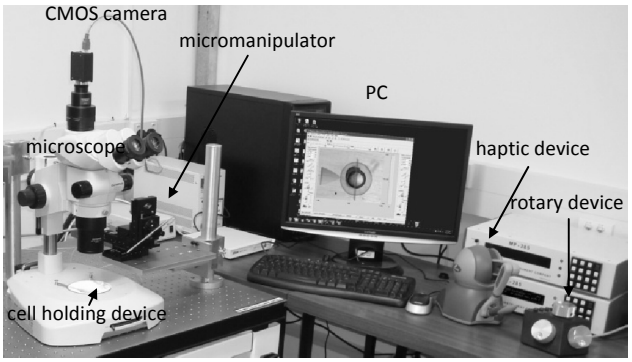

Figure 2. Haptic microrobotic cell injection system.

3 Microrobotic Cell Injection System

The haptically enabled cell injection system setup is shown in Figure 2. The microrobot is the MP-285 micromanipulator from Sutter Instruments providing 3 actuated Degrees of Freedom (DOF) and 2 additional DOF adjustable manually. The 3 actuated DOF each provide a linear range of 25mm with 0.04µm positioning resolution. Cell injection is facilitated through a glass micropipette as shown in Figure 2. A pressure micro-injector system (PMI-200, Dagan) with a computer controlled injection trigger provides positive pressure for material deposition. The cell holding dish is placed in the view of the microscope lens and a CMOS camera (A601f-2, Basler) is mounted on top of the optical microscope (SZX2-ILLB, Olympus) providing the operator with visual information from the cell injection process. A personal computer (Intel Core Duo CPU 2.66GHz, 4GB RAM) is utilised for system control and monitoring. The micromanipulator is interfaced to the PC using a DAQ card (NI PCI-6259) and position feedback is received by the computer's serial port. In order to minimise vibration, the setup (excluding the PC and the injection unit) are mounted on a vibration isolation table.

The developing system focuses on enhancing human-in-the-loop cell injection while retaining the bio-operator's human-level expertise, knowledge and intuition. Feedback from the cell injection process (such as that which would govern a completely autonomous system) is provided to the bio-operator and the bio-operator ultimately decides whether or not to act in accordance with such haptic suggestions. This capability is facilitated by the bilateral nature of the haptic interface. The result is that the bio-operator is provided with system determined suggestions however retains the ability to override such suggestions and exercise its own judgement.

4 Modelling

The micromanipulator's 3 actuated DOF provide a travel range of 25 mm along the corresponding Cartesian axis with maximum speed of 2.9 mm/s. They can be positioned independently and, as such, the micromanipulator is modelled for each individual axis.

Figure 3 illustrates the control system architecture. The controller sends commands to the micromanipulator through a DAQ NI card in the form of voltage level (in range of -2.5 to 2.5 V) and receives the position feedback through the PC serial port.

The system identification problem is to model the behaviour of the microrobotic system where voltage and position along each axis are designated as the system input $u(t)$ and output $y(t)$ respectively.

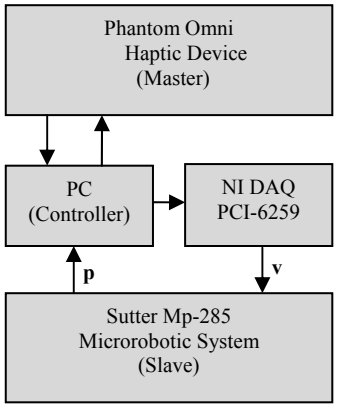

Figure 3. Control system architecture. **v** is the voltage level and **p** is the position feedback.

The first step in system identification is to collect input-output data pairs which represent the behaviour of the system as best as possible. The input was chosen to be a random binary signal shifting between -2.5 and 2.5 V. 3134 input-output data pairs with sampling time of 19.2 ms were collected from the system. Figure 4 shows these input-output data pairs. The collected data pairs were split into two equal sets with equal amount of data for training and checking.

The next step is input selection for the ANFIS model. It is necessary to determine which variables should constitute the input arguments to the ANFIS model. The objective of the system identification is to extract a dynamic process model to predict the output $y(t)$. To achieve this some historical input and output system data is considered as well. The input candidates are partitioned into two disjoint sets as follows:

$$Y = \{y(t\text{-}1), y(t-2), y(t-3), y(t-4)\} \quad (3)$$

$$U = \{u(t\text{-}1), u(t-2), u(t-3), u(t-4), u(t-5), u(t-6)\}$$

As discussed in the previous section, ANFIS uses the hybrid learning method which combines gradient

descent and LSE methods. The LSE method is the major contribution to fast training. In contrast, the gradient descent slowly changes the underlying membership functions which create the basis functions for the LSE method. As a result the ANFIS is able to achieve relatively satisfactory results even after the first training epoch (immediately after the first application of LSE).

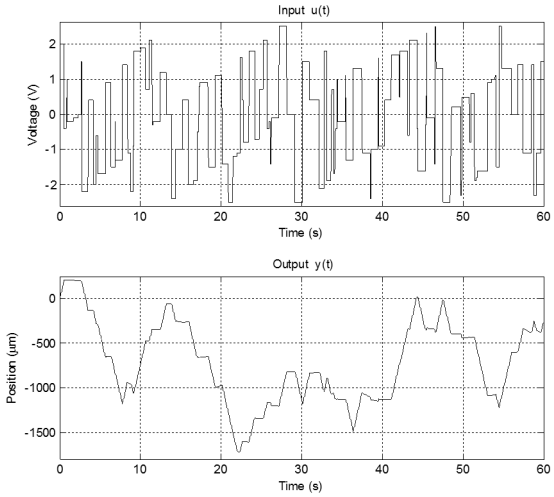

Figure 4. Input-output data pairs.

The LSE method is computationally efficient allowing the construction of ANFIS models with various combinations of input candidates, to run a single training epoch, and to select the one with the best performance based on smallest RMSE (root mean square error).

The heuristic method was employed to select appropriate inputs [Jang, 1996]. In the heuristic approach, all input candidates are treated equally and the best input arguments are selected sequentially. Because there are 10 input candidates, first, 10 ANFIS models with single input of each were constructed. Then, the single input model with the smallest training error was selected. Next, the best model out of 9 possible two-input ANFIS models were chosen. It was observed the three-input ANFIS model provided reasonably low RMSE where beyond this number of inputs, the RMSE did not decrease considerably. As such, the optimum three-input ANFIS model was selected. Next step was to train the network in order to obtain the form of input space partitioning, the members and type of membership functions.

Grid partitioning method was employed to tune the membership functions. The number of fuzzy rules was 2^n where n is the number of input arguments. Each ANFIS model was trained for a single epoch to identify consequent parameters. These parameters indicated each rule's output equation. When n reached to 3, the smallest RMSE of 1.2444 was obtained. It was observed, by proceeding, the RMSE did not decrease considerably any more. As such, the training stopped at this point to avoid unnecessary increase of the input dimension. Figure 5 illustrates error curves for the input selection process for the heuristic approach. The selected inputs are listed according to the order of decreasing training errors.

The ANFIS model output is $y(t)$. The resulted model has 8 fuzzy rules, 34 nodes, 32 consequent parameters and 18 premise parameters. The input selection procedure took 2.23 seconds on a computer with Core Duo CPU 2.66GHz and 4GB RAM.

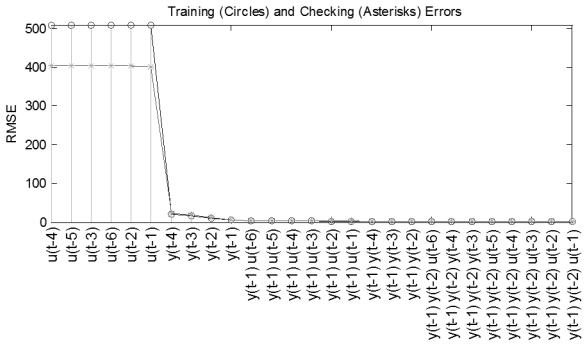

Figure 5. Error curves for input selection in heuristic search.

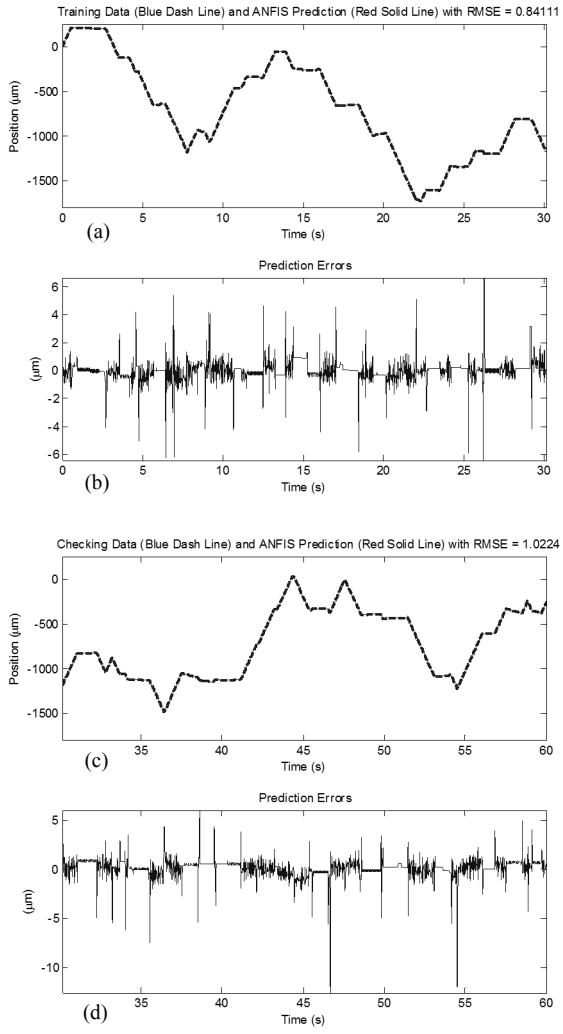

Figure 6. Trained ANFIS model response and corresponding perdition errors.

The next step of the ANFIS model training is to tune premise parameters using the hybrid method. It was observed that after epoch number 5357, RMSE for training data set converged and we stop the training. This is the training stop point. At this point, RMSE for training and checking data set were reduced from 0.9163 to 0.8411 and from 1.0953 to 1.0224 respectively.

Figure 6 (a) demonstrates the response of the model to the training data set. The corresponding prediction errors is very small and is presented in figure 6 (b). Figure 6 (c) demonstrates that while checking data is applied, the trained ANFIS model was able to predict system response precisely. Figure 6 (d) shows the corresponding perdition errors.

As the results indicate, the developed ANFIS model is able to predict the actual system response very precisely with root mean square error of 1.0224 μm while the microrobot moves in cm range (10^4 times).

5 Neuro-Fuzzy Control

To design the controller, the direct inverse learning method [Denai *et al.*, 2007; Psaltis *et al.*, 1988] was employed. Inverse learning or general learning for control was performed in two phases:

- *Learning phase:* the plant ANFIS inverse model was derived based on input-output data pairs generated from the plant ANFIS.
- *Application phase:* the obtained ANFIS inverse model was used to generate the control action.

For the offline mode, a set of training data pairs was collected and the ANFIS network was then trained in the batch mode. For the online mode, in order to deal with time varying dynamics and model inaccuracies, the control actions were generated every *n* time steps while online learning occurs at every time step. Alternatively, it is possible to generate the control sequence at every time step and apply only the first component to the plant. The overall control structure is illustrated in figure 7.

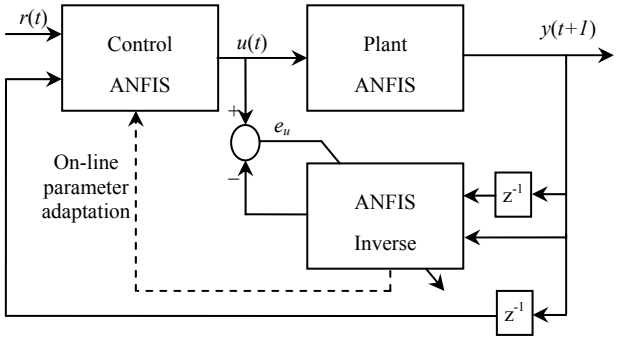

Figure 7. Block diagram of adaptive learning. On-line learning of ANFIS inverse model occurs at each time step to fine-tune the membership function parameters of ANFIS controller.

The premise of inverse control is to drive the plant with a signal from a controller whose transfer function is the inverse of the plant itself. As such, the role of inverse method is to adjust the ANFIS controller parameters to create the plants' inverse ANFIS model.
The plant can be described by

$$y(t+1) = f\,(y(t), u(t)) \tag{4}$$

where $y(t+1)$ is the system state at time $t+1$, $y(t)$ is the system state at time t, and $u(t)$ is the control signal at time t. Accordingly, the state vector at time $t+2$ is

$$y(t+2) = f\,\big(y(t+1), u(t+1)\big) = f\,\big(f\big(y(t), u(t)\big), u(t+1)\big) \tag{5}$$

In general

$$y(t+n) = F\,(y(t), U) \tag{6}$$

where n is the order of the plant, F is a multiple composite function of
f, and U holds the control actions from t to $t+n-1$

$$U = (u(t), u(t+1), \ldots, u(t+n-1))^T \tag{7}$$

The updating expression 6 for y indicates, the sequence of control inputs U drives $y(t)$ to $y(t+n)$ in n time steps. With the assumption of the plant model inverse existence, then U can be expressed as a function of $y(t)$ and $y(t+n)$

$$U = G\,(y(t), y(t+n)) \tag{8}$$

The problem is to find the inverse model G. The ANFIS network is then used to learn the inverse of the plant, G, by fitting the data pairs $(y(t), y(t+1); u(t))$. Then, the training data pairs would be

$$\{\, y(t), y(t+n); U^T\} \tag{9}$$

The learning phase is used to approximate G with G_{est} where the the training data set of expression 9 is collected and applied to train the ANFIS network. After the neuro-fuzzy controller is trained to approximate the inverse dynamic of G, then if the $y(t)$ and the desired reference $r(t+n)$ are given, the neuro-fuzzy controller generates a sequence of control actions

$$U_{est} = G_{est}(y(t), r(t+n)) \tag{10}$$

This control sequence brings $y(t)$ to the desired reference $r(t+n)$ after n steps. 1500 training data sets and 1500 checking data sets were used to develop the ANFIS inverse model. The ANFIS inverse model has 8 fuzzy rules, 34 nodes, 32 consequent parameters and 18 premise parameters. After epoch number 4366, RMSE for the training data set converged. At the end of the learning phase, the RMSE for training and checking data set were reduced from 0.8296 to 0.7462 and from 1.0847 to 1.0153 respectively. This indicates that the inverse model does exist and the direct inverse learning method is capable of accurate approximation.

The developed control scheme was utilized for each of the manipulator's three actuated axes. The control system was implemented on the PC within the VC++ environment deployed from MATLAB©. The controller sends commands to the manipulator through a DAQ NI card in the form of voltage levels and receives the position feedback through the PC's serial port (figure 3).
Figure 8 depicts the controller actual response to the square and sinusoidal wave trajectories in real-time.

The control system needs to approach the desired position as fast as possible with high precision while minimising the overshoot and undershoot. The results indicate the high performance of the control system when approaching the desired position.

Prior to development of the introduced neuro-fuzzy controller, a PID controller was designed and was tuned using the Ziegler-Nichols' (ZN) method. Table 1 compares the PID and NF (neuro-fuzzy) controllers' transient-response characteristics when moving the micromanipulator from P_1 to P_2 as follows

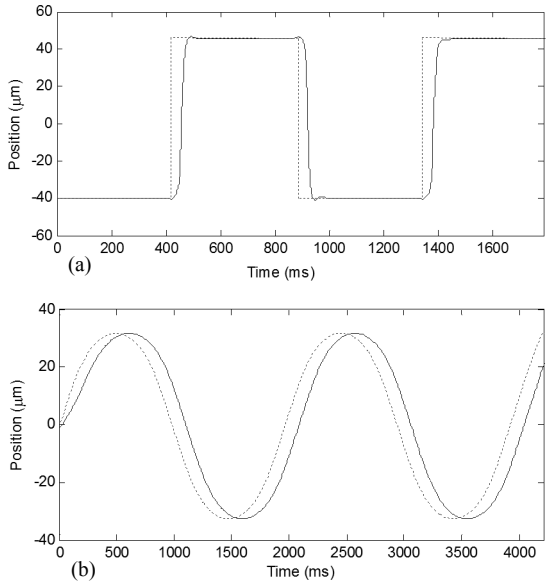

Figure 8. Control system response to the desired trajectory. (a) square wave response in coarse mode (b) Sinusoidal wave response. Dashed red line and solid blue line indicate desired trajectory and control system actual responses respectively.

$$P_1 = \left(P_{1x}, P_{1y}, P_{1z}\right) = \ (696, 162.7, 388)\ \mu m$$
$$P_2 = (P_{2x}, P_{2y}, P_{2z}) \ = \ (429.3, 312, 578.6)\ \mu m \quad (11)$$

As indicated by table 1, the neuro-fuzzy controller achieves higher performance for all transient response characteristics in both the coarse and fine modes. Also, the settling time of the neuro-fuzzy controller is much less than the PID controller. This corresponds to faster positioning and provides less delay for master/slave architecture subject to different scaling factors. The MPO (Maximum Percent Overshoot) is also smaller corresponding to more control precision. The neuro-fuzzy controller shows much higher performance. Given these considerations the neuro-fuzzy controller is the superior choice for micro positioning in this work.

Controller	Axis	P_1 (μm)	P_2 (μm)	$\lvert P_1 - P_2 \rvert$ (μm)	MPO (%)	t_d (ms)	t_r (ms)	t_s (ms)
PID	x	696	429.3	266.7	4.01	180	370	580
NF					2.03	120	230	270
PID	y	312	162.7	149.3	2.54	130	260	440
NF					1.05	100	190	230
PID	z	388	578.6	190.6	3.67	160	320	440
NF					2.01	110	210	240

Table 1. Transient-response characteristics comparison of the PID and neuro-fuzzy controllers. P_1 is the start position, P_2 is the desired position, MPO is the Maximum Percent Overshoot, t_d is the delay time (the time required for the response to reach half the desired value), t_r is the rise time (the time required for the response to reach the desired value) and t_s is the settling time (the time required for the response to reach and stay within %2 of the final value).

6 Conclusion

The haptically enabled system is required to manipulate the microrobot with high accuracy. This requires a control strategy capable of continually repositioning the microrobots' actuated axes whilst maintaining micro precision. This paper addressed the design of a precision control system for the microrobotic cell injection system. As the microrobotic system has an unknown internal structure with nonlinear behaviour, an intelligent dynamic modelling and control scheme was developed. An ANFIS (neuro-fuzzy inference system) and direct inverse learning method were adapted for system identification and control. It was demonstrated that the developed ANFIS model can predict the system's response precisely. Experimental results indicated that the designed intelligent controller provides adequate control characteristics in term of precision and speed which are both important for haptic microrobotic system to perform the cell injection task. This provides the suitable platform for 3D position-to-position kinematic mapping of the haptic/microrobotic system.

References

[Fanning, 2006] G. Fanning, "RNA as a target for host defense and anti-HIV drugs," *Current drug target*, vol. 7, pp. 1607-1613, 2006.

[Beretta, 2006] G. Beretta, P. Perego, and F. Zunino, "Mechanisms of cellular resistance to camptothecins," *Current Medicinal Chemistry*, vol. 13, pp. 3291-3305, 2006.

[Scherp and Hasenstein, 2003] P. Scherp and K. Hasenstein, "Microinjection a tool to study gravitropism," *Advances in Space Research,* vol. 31, pp. 2221-2227, 2003.

[Tran *et al.*, 2003] N. Tran, X. Liu, Z. Yan, D. Abbote, Q. Jiang, E. Kmiec, C. Sigmund, and J. Engelhardt, "Efficiency of chimeraplast gene targeting by direct nuclear injection using a GFP recovery assay," *Molecular Therapy*, vol. 7, pp. 248-253, 2003.

[Kasaya *et al.*, 1999] T. Kasaya, H. Miyazaki, S. Saito, and T. Sato, "Micro object handling under SEM by vision-based automatic control," *IEEE International Conference on Robotics and Automation (ICRA),* pp. 2189-2196, 1999.

[Ghanbari *et al.*, 2009a] A. Ghanbari, W. Wang, C. E. Hann, J. G. Chase, and X. Chen, "Cell image recognition and visual servo control for automated cell injection," *International Conference on Autonomous Robots and Agents,* pp. 92-96, March 2009.

[Faramarzi *et al.*, 2009] S. Faramazi, A. Ghanbari, W. Wang, and X. Chen, "PVDF based 3D force sensor for micro and nano manipulation", *IEEE International Conference on Control & Automation*, pp. 867-871. Feb. 2009.

[Ghanbari *et al.*, 2009b] A. Ghanbari, B. Horen, S. Nahavandi, X. Chen, W. Wang, "Towards haptic microrobotic intracellular injection," *ASME/IEEE MESA conf.*, Aug. 2009.

[Ghanbari, *et al.*, 2010a] A. Ghanbari, X. Chen, W. Wang, B. Horan, H. Abdi and S. Nahavandi, "Haptic microrobotic intracellular injection assistance using virtual fixtures," *11th International Conference on Control Automation Robotics & Vision, 2010*, pp. 781-786.

[Ghanbari, *et al.*, 2010b] A. Ghanbari, H. Abdi, S.

Nahavandi, X, Chen, and W. Wang, "Haptic guidance for microrobotic intracellular injection," *IEEE/RAS-EMBS International Conference on Biomedical Robotics and Biomechatronics*, pp. 162-167, 2010.

[Balijepalli and Kesavadas, 2004] A. Balijepalli and T. Kesavadas, "Value-Addition of Haptics in operator training for complex machining tasks," *Journal of Computing and Information Science in Engineering,* vol. 4, p. 91, 2004.

[Horan *et al.*, 2008a] B. Horan, Z. Najdovski, S. Nahavandi, and E. Tunstel, "Haptic control methodologies for telerobotic stair traversal," *International Journal of Intelligent Control and Systems,* vol. 13, pp. 3-14, 2008.

[Horan *et al.*, 2008b] B. Horan, Z. Najdovski, S. Nahavandi, and E. Tunstel, "3D virtual haptic cone for intuitive vehicle motion control,", *IEEE Symposium on 3D User Interfaces*, pp. 67-74, March 2008.

[Basdogan *et al.*, 2004] C. Basdogan, S. De, J. Kim, M. Muniyandi, H. Kim, and M. Srinivasan, "Haptics in minimally invasive surgical simulation and training," *IEEE Trans. Computer Graphics and Applications,* vol. 24, pp. 56-64, 2004.

[Bai, 2002] E.-W. Bai, "A blind approach to the Hammerstein-Wiener model identification," *Automatica,* vol. 38, no. 6, pp. 967-979, 2002.

[Nauck *et al*., 1997] D. Nauck, F. Klawonn, R. Kruse, *Foundations of Neuro-Fuzzy Systems. Wiley*, New York, 1997.

[Vieira *et al.*, 2004] J. J. Vieira, F. M. Dias, and A. Mota, "Artificial neural networks and neuro-fuzzy systems for modelling and controlling real systems: a comparative study, " *Engineering Applications of Artificial Intelligence,* vol. 17, no. 3, pp. 265-273, 2004.

[Jang, 1993] J. S. R. Jang, "ANFIS: adaptive-network-based fuzzy inference system, " *Systems, Man and Cybernetics, IEEE Transactions on,* vol. 23, no. 3, pp. 665-685, 1993.

[Denai *et al*., 2004] M.A. Denai, F. Palis and A. Zeghbib, "ANFIS based modelling and control of non-linear systems: a tutorial", *IEEE International Conference on Systems, Man and Cybernetics*, vol. 4, pp. 3433-3438, Oct. 2004.

[Jang and Chuen-Tsai, 2002] J.-S.R., Jang and S. Chuen-Tsai, "Neuro-fuzzy modeling and control", *Proceedings of the IEEE*, vol. 83, pp. 378-406, Aug. 2002.

[Jang *et al.*, 1997] J. S. Jang, C. T. Sun, E. Mizutani, *Neuro-fuzzy and soft computing*, Prentice Hall, NJ, 1997.

[Takagi and Sugeno, 1985] T. Takagi and M. Sugeno, "Fuzzy identification of systems and its applications to modeling and control", *Systems, Man and Cybernetics, IEEE Transactions on,* vol. 15, pp. 116-132, 1985.

[Ghanbari *et al.*, 2009c] A. Ghanbari, X. Chen and W. Wang, "Neuro-fuzzy microrobotic system identification for haptic intracellular injection," *IEEE International Conference on Control & Automation*, pp. 860-866, Feb. 2009.

[Jang, 1996] J-S. R. Jang, "Input selection for ANFIS learning"*, IEEE International Conference on Fuzzy Systems*, vol. 2, pp. 1493-1499, Sep. 1996.

[Denai *et al.*, 2007] M.A. Denai, F. Palis and A. Zeghbib, "Modeling and control of non-linear systems using soft computing techniques," *Journal of Applied Soft Computing*, *Elsevier*, vol. 7, pp. 728-738, 2007.

[Psaltis *et al.*, 1988] D. Psaltis, A. Sideris and A.A. Yamamura, "A multilayered neural network controller," *IEEE Control Systems Magazine*, vol. 8, pp. 17-21, 1988.